

## Supporting Information

### Realizing high-rate aqueous zinc-ion battery using organic cathode material containing electron withdrawing group

Xiaojuan Chen<sup>a</sup>, Haoqi Su<sup>a</sup>, Baozhu Yang<sup>a</sup>, Gui Yin<sup>b</sup>, Qi Liu<sup>a,b\*</sup>

<sup>a</sup>Jiangsu Key Laboratory of Advanced Catalytic Materials and Technology, Advanced Catalysis Green Manufacturing Collaborative Innovation Center and School of Petrochemical Engineering, Changzhou University, 1 Gehu Road, Changzhou, Jiangsu 213164, China.

<sup>b</sup>State Key Laboratory of Coordination Chemistry, Nanjing University, Nanjing, Jiangsu 210093, China.

### Table of Contents

No	Title	Page
1	<b>Supporting Figures and Tables</b>	P3
	<b>Figure S1.</b> Synthetic route of HFHATN	P3
	<b>Figure S2.</b> Liquid state <sup>1</sup> H NMR of HFHATN.	P3
	<b>Figure S3.</b> Solid state <sup>13</sup> C NMR of HFHATN.	P3
	<b>Figure S4.</b> Mass spectra of HFHATN.	P4
	<b>Figure S5.</b> FTIR spectra of HFHATN.	P4
	<b>Figure S6.</b> XRD spectra of HFHATN.	P4
	<b>Figure S7.</b> FESEM images of HFHATN samples.	P5
	<b>Figure S8.</b> Rate capability of HFHATN electrodes.	P5
	<b>Figure S9.</b> The performance of different loading of HFHATN electrode.	P5
	<b>Figure S10.</b> Nyquist plot of EIS measurement for the Zn//HFHATN battery.	P6
	<b>Figure S11.</b> Self-discharge behavior tested of HFHATN electrode.	P6
	<b>Figure S12.</b> Ex-situ XPS spectra of HFHATN electrode	P7
	<b>Figure S13.</b> Ex-situ FT-IR spectra of HFHATN electrode.	P7
	<b>Figure S14.</b> Solid-state <sup>1</sup> H NMR spectra of the HFHATN electrode	P8
	<b>Figure S15.</b> XRD patterns of the pristine electrode and the discharge electrode and Zn <sub>4</sub> (OH) <sub>6</sub> SO <sub>4</sub> ·5H <sub>2</sub> O	P8
	<b>Figure S16.</b> The images of the assembled flexible aqueous Zn//HFHATN battery.	P9
	<b>Figure S17.</b> The rate performances of flexible aqueous Zn//HFHATN	P9

	battery.	
	<b>Figure S18.</b> The energy density and power density of the flexible Zn//HFHATN battery.	<b>P10</b>
	<b>Figure S19.</b> Flexible performance of the flexible Zn//HFHATN battery at bending degrees.	<b>P10</b>
	<b>Table S1.</b> Comparison of maximum specific capacity in aqueous zinc batteries.	<b>P11</b>
	<b>Table S2.</b> Sum of electronic and zero-point energies in hartree calculated at the B3LYP/6-31+G (d, p) level.	<b>P12</b>
	<b>Table S3.</b> Comparison of energy and power densities between present work and previous reported flexible batteries and supercapacitors.	<b>P12</b>
<b>2</b>	<b>Note</b>	
2.1	<b>Calculation about energy density and power density for Zn full batteries and flexible Zn batteries</b>	<b>P13</b>
2.2	<b>Calculation about the capacity contribution ratio from Zn<sup>2+</sup> and H<sup>+</sup> based on inductively coupled plasma atomic emission spectroscopy (ICP-AES)</b>	<b>P14</b>
<b>3</b>	<b>References</b>	<b>P15</b>

## 1. Supporting Figures and Tables

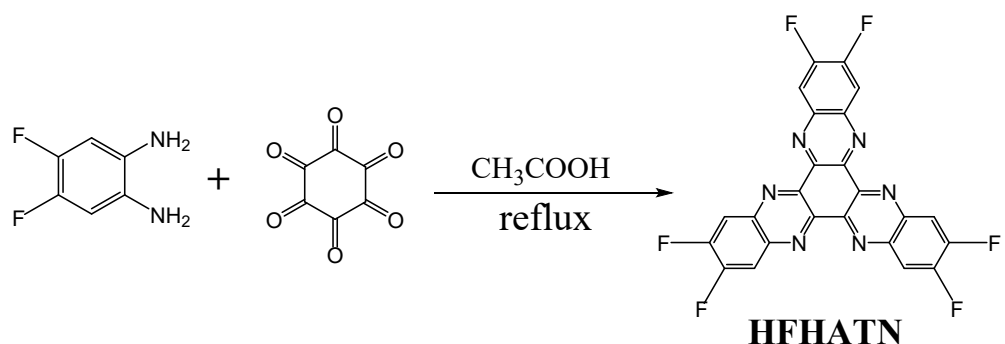


**Figure S1.** Synthetic route of HFHATN.

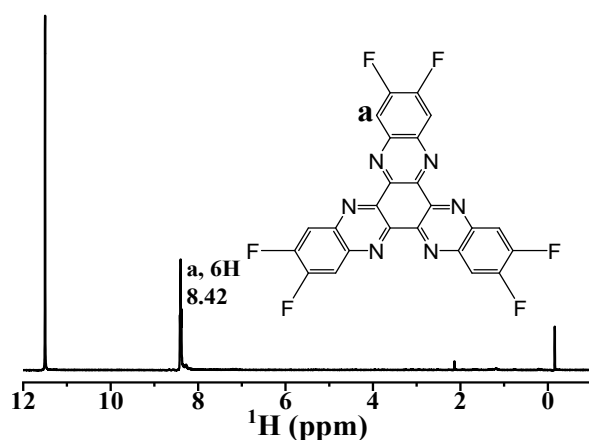


**Figure S2.** Liquid state  $^1\text{H}$  NMR spectrum of HFHATN.

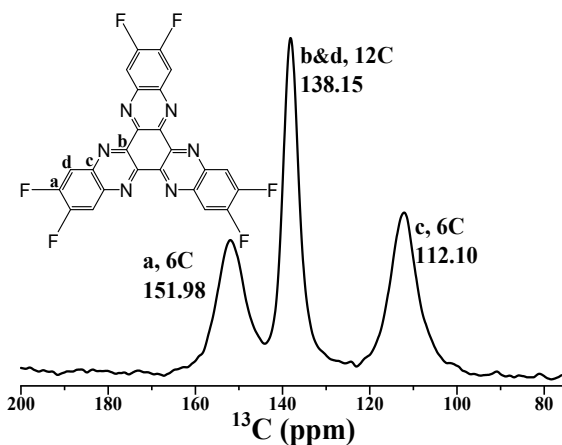


**Figure S3.** Solid state  $^{13}\text{C}$  NMR spectrum of HFHATN.

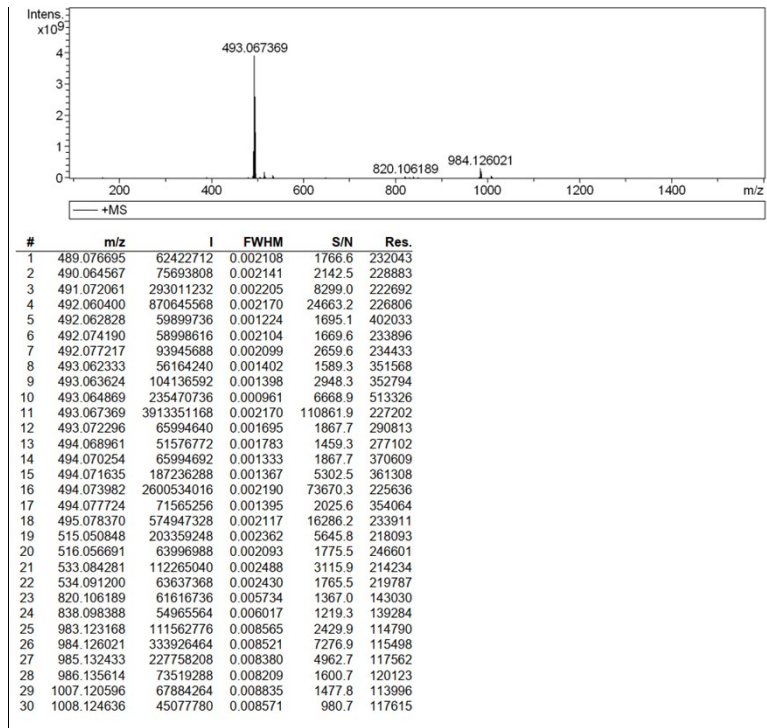


**Figure S4.** Mass spectrum of HFHATN.

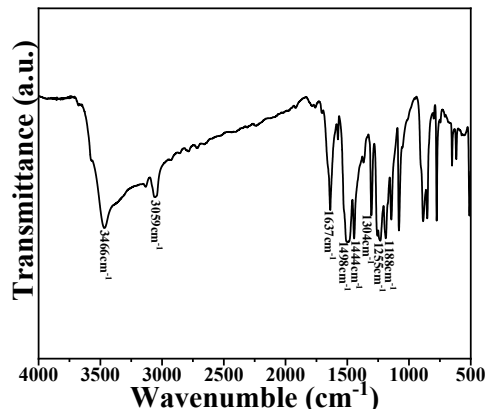


**Figure S5.** FTIR spectrum of HFHATN.

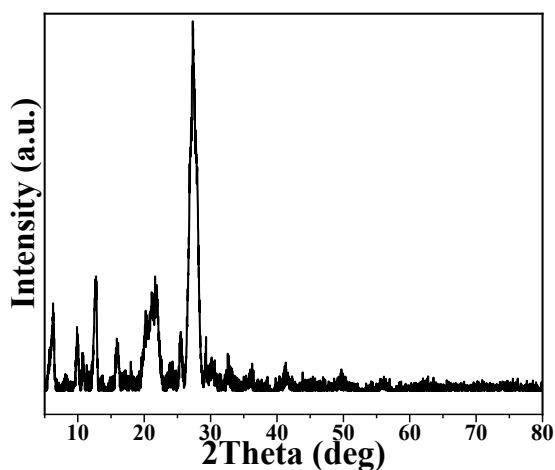


**Figure S6.** XRD spectrum of HFHATN.

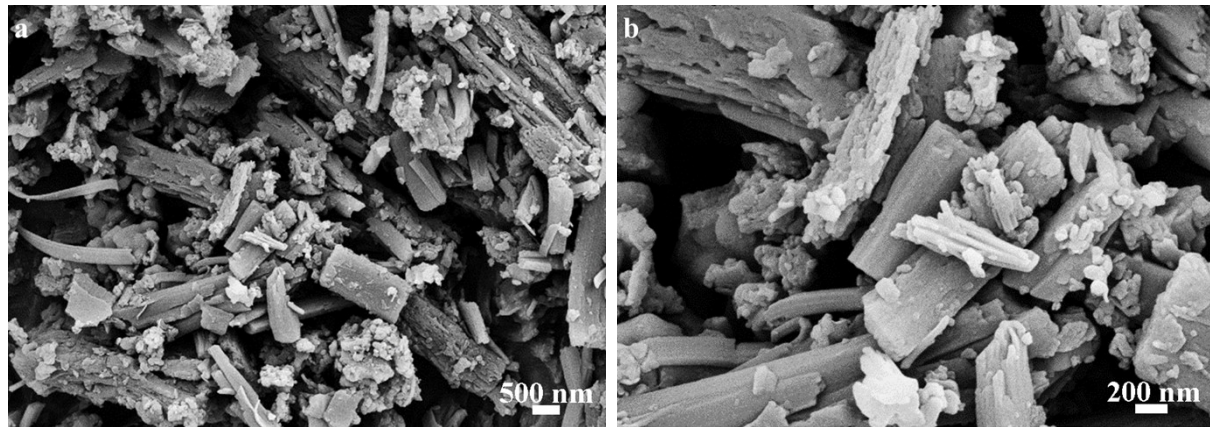


**Figure S7.** FESEM images of the HFHATN material (a) lower magnification (b) higher magnification.

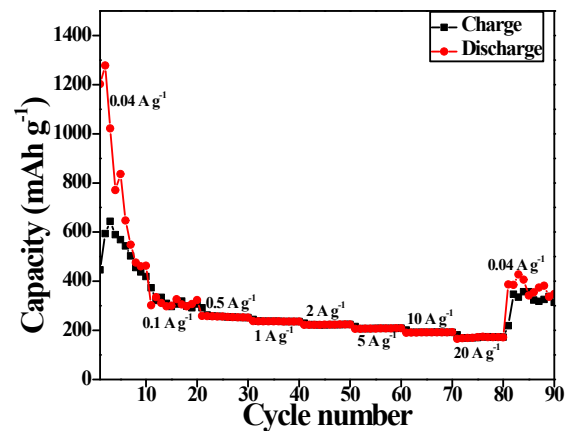


**Figure S8.** Rate capability of HFHATN electrode at various current densities.

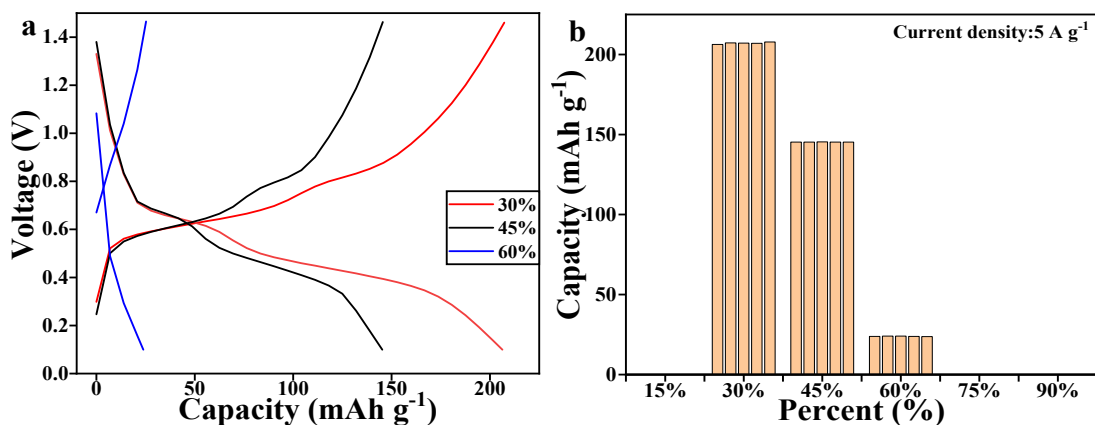


**Figure S9.** Galvanostatic discharge/charge curves (a) and discharge histogram (b) of HFHATN electrode with different loading of active materials at a current density of  $5 \text{ A g}^{-1}$ .

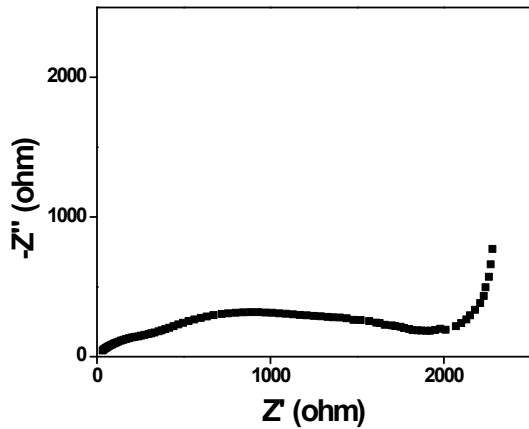


**Figure S10.** Nyquist plot of EIS measurement for the Zn//HFHATN battery.

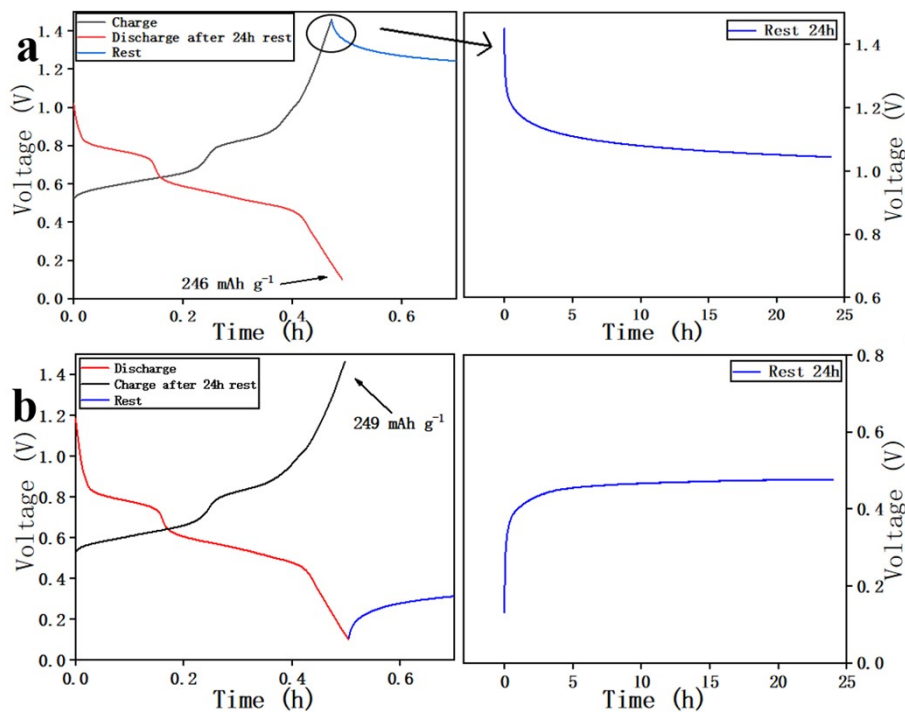


**Figure S11.** Self-discharge behavior tested of HFHATN electrode at a current density of  $0.5\text{A g}^{-1}$ , (a) when firstly charged to 1.46 V, and then discharged to 0.1 V after rest for 24 hours, and (b) when firstly discharged to 0.1 V, and then charged to 1.46 V after rest for 24 hours

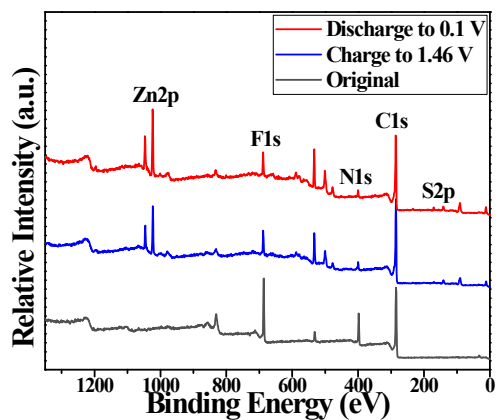


**Figure S 12.** Ex-situ XPS spectra of HFHATN electrode at pristine, fully discharged (0.1 V) and fully charged (1.46 V) states in a discharge/charge cycle. An aqueous coin battery was tested at a current density of  $0.5 \text{ A g}^{-1}$  for examination.

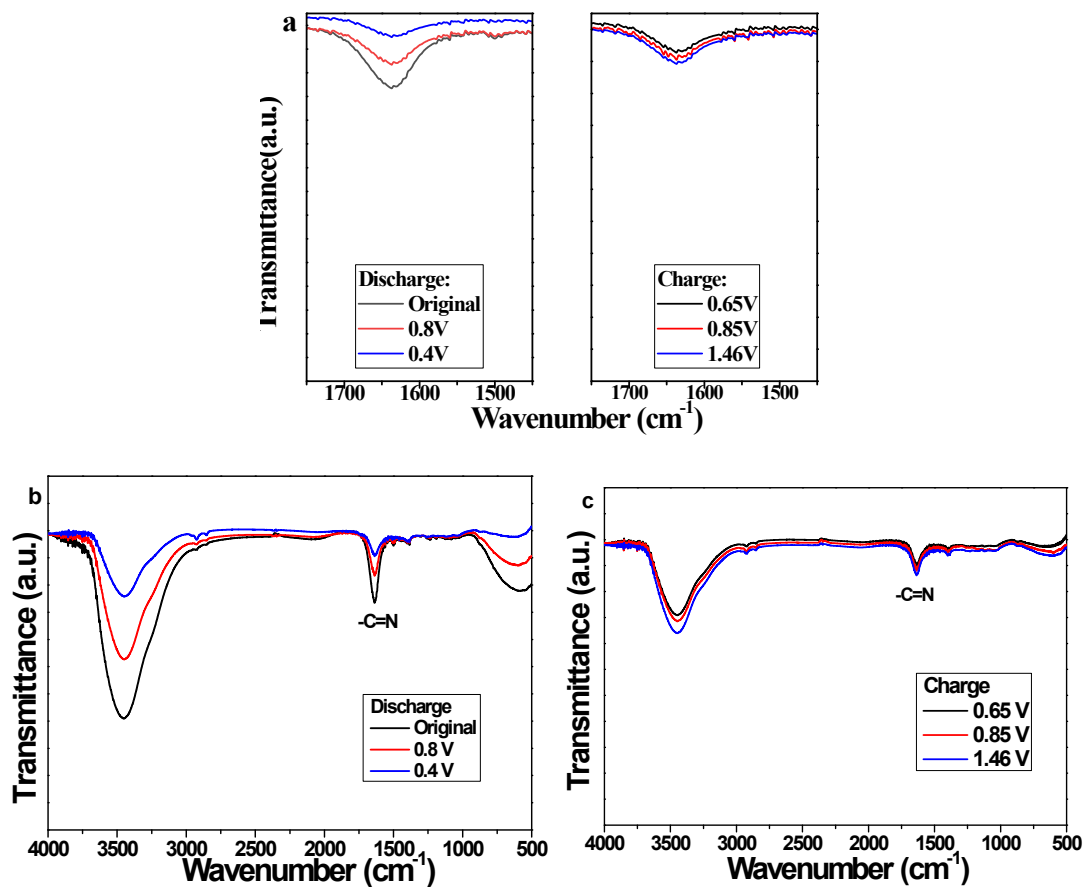


**Figure S 13.** Ex-situ FT-IR spectra of HFHATN electrode (a, b, c) at pristine, fully discharged (0.1 V) and fully charged (1.46 V) states in a discharge/charge cycle. An aqueous coin cell was tested at a current density of  $0.5 \text{ A g}^{-1}$  for examination.

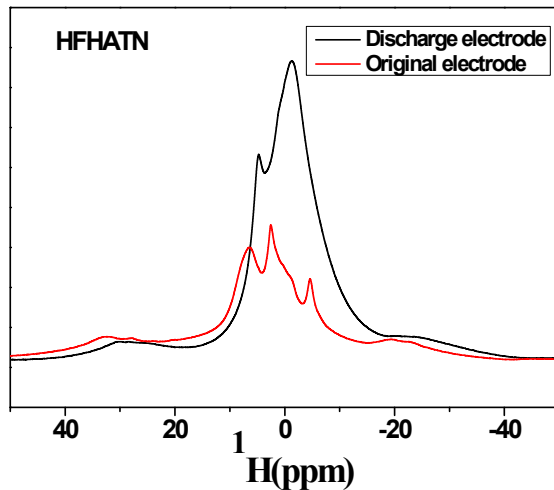


**Figure S14.** Solid-state  $^1\text{H}$  NMR spectra of the HFHATN electrode under the original and discharge conditions

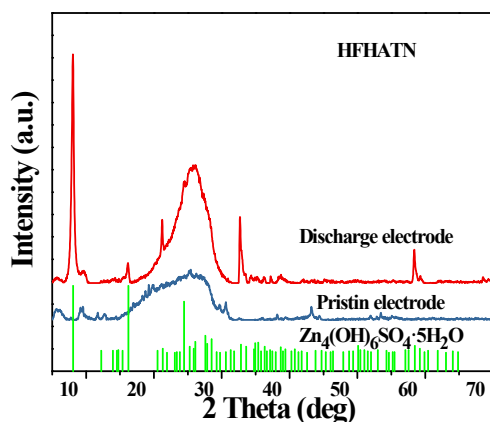


**Figure S15.** XRD patterns of the pristine electrode and the discharge electrode and  $\text{Zn}_4(\text{OH})_6\text{SO}_4 \cdot 5\text{H}_2\text{O}$  (PDF no 39-0688)

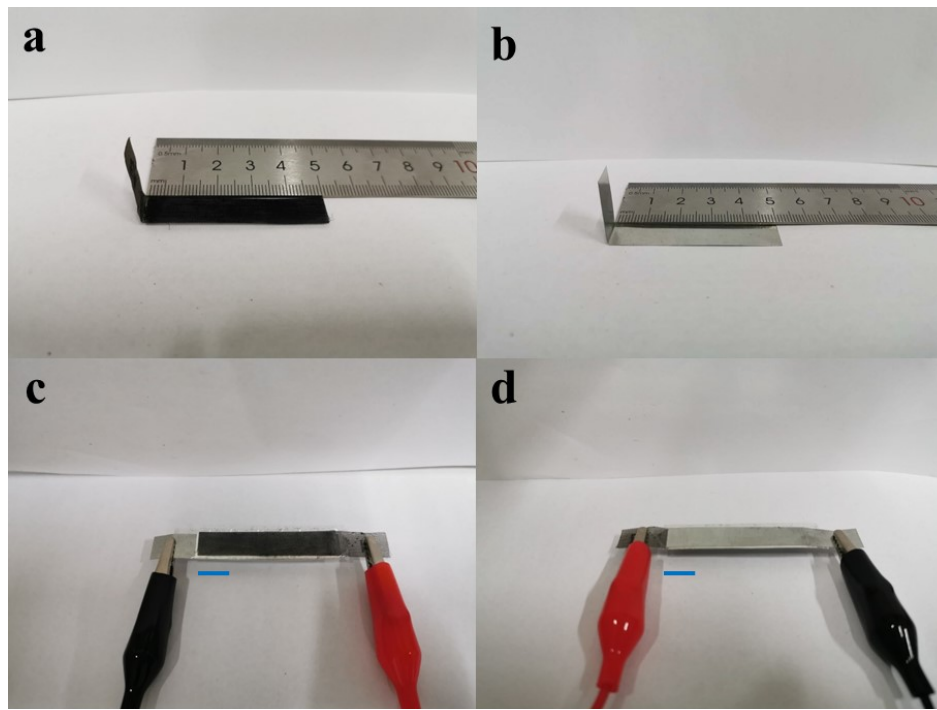


**Figure S16.** The images of the assembled flexible aqueous Zn//HFHATN battery. HFHATN cathode material (a) and Zn foil (b) in size of 1cm × 5 cm. The cathode-side-view (c) and the anode-side-view (d) of the flexible battery. (scale bar: 1cm)

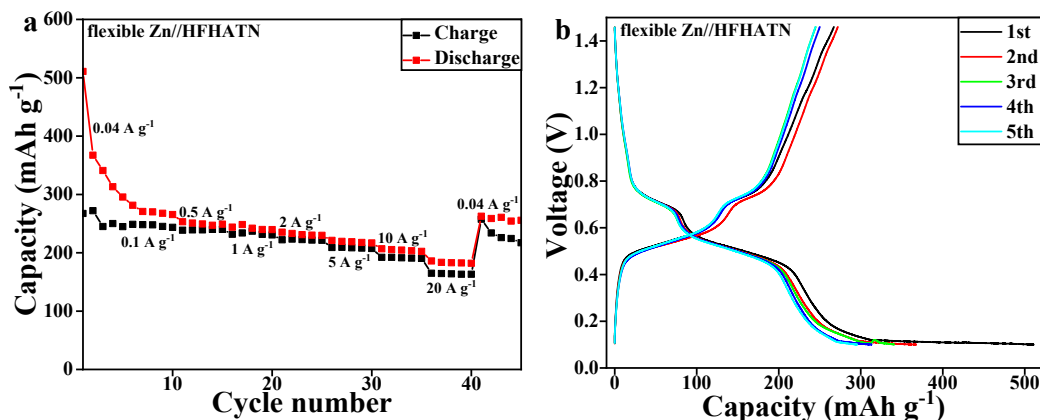


**Figure S17.** (a) The rate performances of flexible aqueous Zn//HFHATN battery. (b) The galvanostatic discharge/charge curves of flexible aqueous Zn//HFHATN battery at a current density of 0.04 A g<sup>-1</sup>.

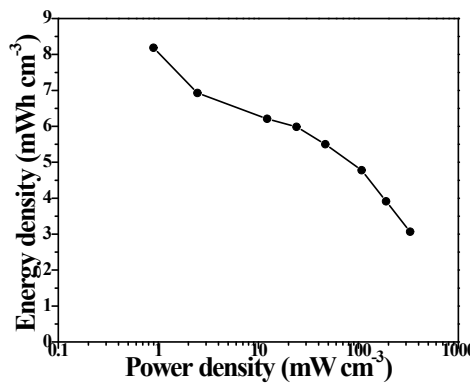


**Figure S18.** The Ragone plot of the flexible Zn//HFHATN battery.

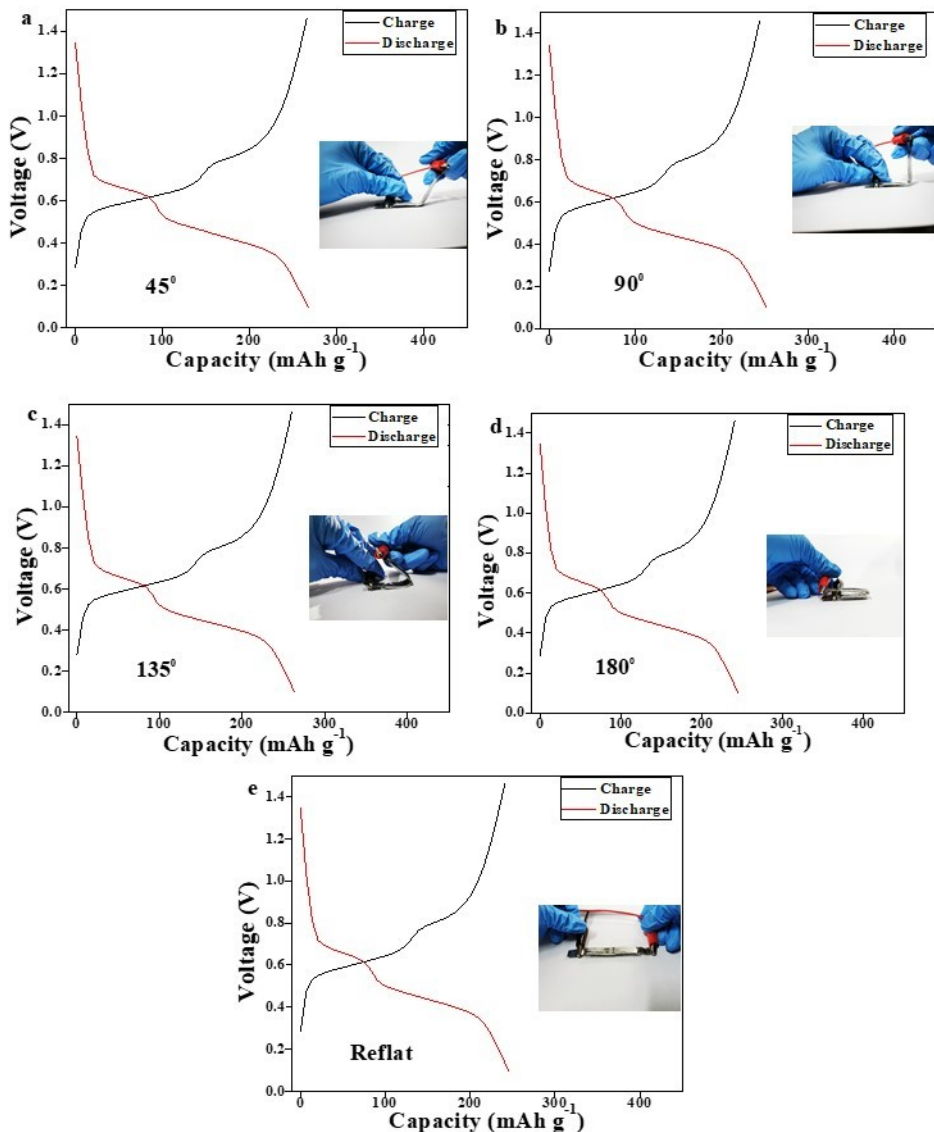


**Figure S19** Flexible performance of the flexible Zn//HFHATN battery at bending degrees of (a)  $45^\circ$ , (b)  $90^\circ$  (c)  $135^\circ$ , (d)  $180^\circ$  and (e) reflat. The insets are optical images of the flexible aqueous battery at corresponding bending degrees.

**Table S1.** Comparison of specific capacity in aqueous zinc batteries.

Electrode Materials	Specific capacity (Current density) /mA h g <sup>-1</sup> (mA g <sup>-1</sup> )	Voltage / (V vs Zn/Zn <sup>2+</sup> )	Refs.
Quinone(C4Q)	333 (50)	0.8—1.3 V	24
Pyrene-4,5,9,10-tetraone	336 (40)	0.36—1.46V	25
p-chloranil	>200 (217)	0.8—1.4V	23
DTT	211/97 (50/2000)	0.3-1.4 V	27
NDI	~200/~25(0.2/10 C)	0.2-1.0 V	28
HATN	963/174 (40/6000)	0.1—1.46V	32
HMHATN	542/115 (40/8000)	0.1—1.46V	32
HATN	405/123 (100/20000)	0.3-1.1 V	33
HATN-3CN	313/190 (50/20000)	0.1-1.6 V	34
TCNAQ	166/55(50/1000)	0.6-1.8 V	35
PQ-Δ	225/210 (30/150)	0.25-1.6 V	29
PDB	205/176 (50 /1000)	0.2-1.55	30
PA-COF	265/68 (50/10000)	0.2-1.6 V	36
BDB	125 (25)	0.6-1.8 V	S1
PC/G-2	355/ 171 (50/5000)	0.2-1.9 V	S2
PANI	184/110 (20/10000)	0.5-1.6 V	S3
PANI	200/ 89 (50/5000)	0.5-1.5 V	S4
PDA	126.2/43.2(20/5000)	0.3-1.4 V	S5
PBQS	203/126 (20/1000)	0.2-1.8 V	S6
HqTp	276/125 (85/3750)	0.2-1.8 V	S7
HFHATN	461/172 (40/20000)	0.1-1.46 V	This work

Refs. 19- ---30 was given in the main-text

**Table S2** Sum of electronic and zero-point energies in hartree calculated at the B3LYP/6-31+G (d, p) level.

	Energy/Hartree
Zn	-1779.1040434
H	-0.2151804
HFHATN	-1845.7542577
HFHATN_3Zn	-7183.21715873

1hartree =2625.5kJ/mol =27.21eV=627.51kcal/mol

**Table S3.** Comparison of energy and power densities between present work and previous reported flexible batteries and supercapacitors.

Flexible Materials	Energy Density (mWh cm <sup>-3</sup> )	Power Density (W cm <sup>-3</sup> )	Refs.
HZnO@MnO <sub>2</sub> SSC	0.04	0.00024	S8
MWCNT/CMF SSC	0.14	0.0027	S9
H-TiO <sub>2</sub> @MnO <sub>2</sub> //H-TiO <sub>2</sub> @C ASC	0.30	0.23	S10
Graphite/PANI SSC	0.32	0.054	S11
MVNN/CNT SSC	0.54	0.43	S12
MnO <sub>2</sub> /Fe <sub>2</sub> O <sub>3</sub> ASC	0.55	0.139	S13
VO <sub>x</sub> /VN ASC	0.61	0.85	S14
Co <sub>3</sub> O <sub>4</sub> //graphene ASC	0.62	1.47	S15
ppy-coated paper SSC	1	0.27	S16
WO <sub>3-x</sub> /MoO <sub>3-x</sub> //PANI ASC	1.9	0.73	S17
Ni(OH) <sub>2</sub> NM//OMC fibers ASC	2.16	1.6	S18
PANI/Au ASC	10	3	S19
MWCNT//Li <sub>4</sub> Ti <sub>5</sub> O <sub>12</sub> ASC	3.85	0.565	S20
ppy-MnO <sub>2</sub> -CF SSC	6.16	0.4	S21
SWCNT/N-rGO microfibers SSC	6.3	1.085	S22
LiMn <sub>2</sub> O <sub>4</sub> //Li <sub>4</sub> Ti <sub>5</sub> O <sub>12</sub> planar battery	10	---	S23
LiCoO <sub>2</sub> //LiPON//Li battery	2.2	---	S24
LiMn <sub>2</sub> O <sub>4</sub> //Li <sub>4</sub> Ti <sub>5</sub> O <sub>12</sub> wire battery	17.7	0.56	S25
Na <sub>0.44</sub> MnO <sub>2</sub> //NaTi <sub>2</sub> (PO <sub>4</sub> ) <sub>3</sub> battery	23.8	3.8	S26
Li <sub>1.1</sub> Mn <sub>2</sub> O <sub>4</sub> //LiTi <sub>2</sub> (PO <sub>4</sub> ) <sub>3</sub> battery	124	11.1	S27
Zn//Ni-NiO@CF battery	0.67	---	S28
ZnO@CC//NiO@CC battery	7.76	0.54	S29

PTO//Zn battery	38.72	1.70	25
HATN//Zn battery	22.9	0.069	32
HMHATN//Zn battery	19.2	0.067	32
HFHATN//Zn battery	8.2	0.33	This work

**Note:** In the above table, *ASC* represents “asymmetric supercapacitor”, and *SSC* represents “symmetric supercapacitor”. In addition, Refs. 25 and 32 were given in the main-text. Refs. S1 to S29 are given in following Supplemental References section.

## 2. Note

### 2.1 Calculation about energy density and power density for Zn full batteries and flexible Zn batteries

In the main text, the current densities and specific capacities are calculated according to the mass of the active organic materials in the cathode. The detailed calculation about energy density and power density of Zn full batteries and flexible Zn batteries are presented as follows:

1. Calculation of the discharge capacity (mA h): The discharge specific capacity (mA h g<sup>-1</sup>) multiplied by the mass of the active materials (m, g).

$$C = \text{Specific capacity} \times m \quad (1)$$

2. The calculation of the consumed zinc foil quality (g): The discharge capacity (mA h) was divided by the theoretical specific capacity of zinc (820 mA h/g).

$$m(\text{Zn}) = C/820 \quad (2)$$

3. Calculation of the energy density of Zn full/flexible battery is based following equation:

$$E = C \times V \times 1000/m \quad (3)$$

Where E, C, V and m stand for energy density (Wh kg<sup>-1</sup>), the discharge capacity (mAh), the average discharge voltage (V) and the total mass of the cathode (active organic material) and anode (the consumed Zn) (kg), respectively.

4. Calculation of the power density of Zn full/flexible battery is based following equation:

$$P = E/t \quad (4)$$

Where P is the power density ( $\text{W kg}^{-1}$ ), E is the energy density ( $\text{Wh kg}^{-1}$ ) and t is the discharge time (h).

5. Calculation of the volume energy density of flexible Zn battery is based following equation:

$$E_{\text{vol}} = C \times V/v \quad (5)$$

Where  $E_{\text{vol}}$ , C, V and v stand for the volume energy density ( $\text{mWh cm}^{-3}$ ), the discharge capacity (mAh), the average discharge voltage (V), and the volume of the flexible Zn battery ( $\text{cm}^3$ ), respectively.

6. Calculation of the volume power density of flexible Zn battery is based following equation:

$$P = E_{\text{vol}} / t \quad (6)$$

Where P is the volume power density ( $\text{mW cm}^{-3}$ ),  $E_{\text{vol}}$  is the volume energy density ( $\text{mWh cm}^{-3}$ ) and t is the discharge time (h).

## 2.1 Calculation about the capacity contribution ratio from $\text{Zn}^{2+}$ and $\text{H}^+$ based on inductively coupled plasma atomic emission spectroscopy (ICP-AES)

*Mass ratio of Zn and S* = 53978.7 : 1681

$$\text{Mass ratio of Zn and S} = \frac{53978.7}{65.39} : \frac{1682}{32.065}$$

*Molar ratio of coordinated  $\text{Zn}^{2+}$  and  $\text{Zn}_4(\text{OH})_6\text{SO}_4 \cdot \text{H}_2\text{O}$*

$$= \left( \frac{53978.7}{65.39} - 4 * \frac{1682}{32.065} \right) : \frac{1682}{32.065}$$

*Molar ratio of coordinated  $\text{Zn}^{2+}$  and  $\text{H}^+$*

$$= \left( \frac{53978.7}{65.39} - 4 * \frac{1682}{32.065} \right) : \left( 6 * \frac{1682}{32.065} \right)$$

*Capacity contribution ratio from  $\text{Zn}^{2+}$  and  $\text{H}^+$*

$$= 2 * \left( \frac{53978.7}{65.39} - 4 * \frac{1682}{32.065} \right) : \left( 6 * \frac{1682}{32.065} \right)$$

Based on above calculation, the capacity contribution from Zn<sup>2+</sup> is about 79.7% and that from H<sup>+</sup> is about 20.3%.

### 3. References

- S1. H. Glatz, E. Lizundia, F. Pacifico and D. Kundu, *ACS Appl. Energy Mater.*, 2019, **2**, 1288-1294.
- S2. S. Zhang, W. Zhao, H. Li and Q. Xu, *ChemSusChem*, 2020, **13**, 188-195.
- S3. H. Y. Shi, Y. J. Ye, K. Liu, Y. Song and X. Sun, *Angew. Chem. Int. Ed.*, 2018, **57**, 16359-16363.
- S4. F. Wan, L. Zhang, X. Wang, S. Bi, Z. Niu and J. Chen, *Adv. Funct. Mater.*, 2018, **28**, 1804975.
- S5. X. Yue, H. Liu and P. Liu, *Chem. Commun.*, 2019, **55**, 1647-1650.
- S6. G. Dawut, Y. Lu, L. Miao and J. Chen, *Inorg. Chem. Front.*, 2018, **5**, 1391-1396.
- S7. A. Khayum, M. Ghosh, V. Vijayakumar, A. Halder, M. Nurhuda, S. Kumar, M. Addicoat, S. Kurungot and R. Banerjee, *Chem. Sci.*, 2019, **10**, 8889-8894
- S8. P. Yang, X. Xiao, Y. Li, Y. Ding, P. Qiang, X. Tan, W. Mai, Z. Lin, W. Wu, T. Li, H. Jin, P. Liu, J. Zhou, C. P. Wong and Z. L. Wang, *ACS Nano.*, 2013, **7**, 2617-2626.
- S9. V. T. Le, H. Kim, A. Ghosh, J. Kim, J. Chang, Q. A. Vu, D. T. Pham, J. H. Lee, S. W. Kim and Y. H. Lee, *ACS Nano.*, 2013, **7**, 5940-5947.
- S10. X. Lu, M. Yu, G. Wang, T. Zhai, S. Xie, Y. Ling, Y. Tong and Y. Li, *Adv. Mater.*, 2013, **25**, 267-272.
- S11. B. Yao, L. Yuan, X. Xiao, J. Zhang, Y. Qi, J. Zhou, J. Zhou, B. Hu and W. Chen, *Nano Energy.*, 2013, **2**, 1071-1078.
- S12. X. Xiao, X. Peng, H. Jin, T. Li, C. Zhang, B. Gao, B. Hu, K. Huo and J. Zhou, *Adv. Mater.*, 2013, **25**, 5091-5097.
- S13. P. Yang, Y. Ding, Z. Lin, Z. Chen, Y. Li, P. Qiang, M. Ebrahimi, W. Mai, C. P. Wong and Z. L.

- Wang. *Nano Lett.*, 2014, **14**, 731-736.
- S14. X. Lu, M. Yu, T. Zhai, G. Wang, S. Xie, T. Liu, C. Liang, Y. Tong and Y. Li. *Nano Lett.*, 2013, **13**, 2628-2633.
- S15. X. Wang, B. Liu, R. Liu, Q. Wang, X. Hou, D. Chen, R. Wang and G. Shen, *Angew. Chem. Int. Ed.*, 2014, **53**, 1849-1853.
- S16. L. Yuan, B. Yao, B. Hu, K. Huo, W. Chen and J. Zhou, *Energy Environ Sci.*, 2013, **6**, 470.
- S17. X. Xiao, T. Ding, L. Yuan, Y. Shen, Q. Zhong, X. Zhang, Y. Cao, B. Hu, T. Zhai, L. Gong, J. Chen, Y. Tong, J. Zhou and Z. L. Wang, *Adv. Energy Mater.*, 2012, **2**, 1328-1332.
- S18. X. Dong, Z. Guo, Y. Song, M. Hou, J. Wang, Y. Wang and Y. Xia, *Adv. Funct. Mater.*, 2014, **24**, 3405-3412.
- S19. L. Yuan, X. Xiao, T. Ding, J. Zhong, X. Zhang, Y. Shen, B. Hu, Y. Huang, J. Zhou and Z. L. Wang, *Angew. Chem. Int. Ed.*, 2012, **51**, 4934-4938.
- S20. W. Zuo, C. Wang, Y. Li and J. Liu, *Sci. Rep.*, 2015, **5**, 7780.
- S21. J. Tao, N. Liu, W. Ma, L. Ding, L. Li, J. Su and Y. Gao, *Sci. Rep.*, 2013, **3**, 2286.
- S22. D. Yu, K. Goh, H. Wang, L. Wei, W. Jiang, Q. Zhang, L. Dai and Y. Chen, *Nat. Nanotechnology.*, 2014, **9**, 555-562.
- S23. Y. Yang, S. Jeong, L. Hu, H. Wu, S. W. Lee and Y. Cui, *P. Natl. Acad. Sci. USA.*, 2011, **108**, 13013-13018.
- S24. M. Koo, K. I. Park, S. H. Lee, M. Suh, D. Y. Jeon, J. W. Choi, K. Kang and K. J. Lee, *Nano Lett.*, 2012, **12**, 4810-4816.
- S25. J. Ren, Y. Zhang, W. Bai, X. Chen, Z. Zhang, X. Fang, W. Weng, Y. Wang and H. Peng, *Angew. Chem. Int. Ed.*, 2014, **53**, 7864-7869.

- S26. Z. Guo, Y. Zhao, Y. Ding, X. Dong, L. Chen, J. Cao, C. Wang, Y. Xia, H. Peng and Y. Wang, *Chem.*, 2017, **3**, 348-362.
- S27. X. Dong, L. Chen, X. Su, Y. Wang and Y. Xia, *Angew. Chem. Int. Ed.*, 2016, **128**, 7600-7603.
- S28. Y. Zeng, Y. Meng, Z. Lai, X. Zhang, M. Yu, P. Fang, M. Wu, Y. Tong, and X. Lu, *Adv. Mater.*, 2017, **29**, 1702698
- S29. J. Liu, C. Guan, C. Zhou, Z. Fan, Q. Ke, G. Zhang, C. Liu, and J. Wang, *Adv. Mater.*, 2016, **28**, 8732-8739.